the FEBS Journal

Structural and functional effects of two stabilizing substitutions, D137L and G126R, in the middle part of α-tropomyosin molecule

Alexander M. Matyushenko[1], Natalia V. Artemova[1], Daniil V. Shchepkin[2], Galina V. Kopylova[2], Sergey Y. Bershitsky[2], Andrey K. Tsaturyan[3,4], Nikolai N. Sluchanko[1] and Dmitrii I. Levitsky[1,5]

1 A. N. Bach Institute of Biochemistry, Russian Academy of Sciences, Moscow, Russia
2 Institute of Immunology and Physiology, Russian Academy of Sciences, Yekaterinburg, Russia
3 Institute of Mechanics, Moscow State University, Russia
4 A. A. Blagonravov Institute of Machines Science, Russian Academy of Sciences, Moscow, Russia
5 A. N. Belozersky Institute of Physico-chemical Biology, Moscow State University, Russia

Keywords
actin–myosin interaction; Ca^{2+} regulation of muscle contraction; coiled-coil stabilization; flexibility; *in vitro* motility assay; tropomyosin

Correspondence
D. I. Levitsky, A. N. Bach Institute of Biochemistry, Russian Academy of Sciences, Leninsky prosp. 33, 119071 Moscow, Russia
Fax: (+7) 495 954 2732
Tel: (+7) 495 952 1384.
E-mail: levitsky@inbi.ras.ru

(Received 15 October 2013, revised 15 January 2014, accepted 12 February 2014)

doi:10.1111/febs.12756

Tropomyosin (Tm) is an α-helical coiled-coil protein that binds along the length of actin filament and plays an essential role in the regulation of muscle contraction. There are two highly conserved non-canonical residues in the middle part of the Tm molecule, Asp137 and Gly126, which are thought to impart conformational instability (flexibility) to this region of Tm which is considered crucial for its regulatory functions. It was shown previously that replacement of these residues by canonical ones (Leu substitution for Asp137 and Arg substitution for Gly126) results in stabilization of the coiled-coil in the middle of Tm and affects its regulatory function. Here we employed various methods to compare structural and functional features of Tm mutants carrying stabilizing substitutions Arg137Leu and Gly126Arg. Moreover, we for the first time analyzed the properties of Tm carrying both these substitutions within the same molecule. The results show that both substitutions similarly stabilize the Tm coiled-coil structure, and their combined action leads to further significant stabilization of the Tm molecule. This stabilization not only enhances maximal sliding velocity of regulated actin filaments in the *in vitro* motility assay at high Ca^{2+} concentrations but also increases Ca^{2+} sensitivity of the actin–myosin interaction underlying this sliding. We propose that the effects of these substitutions on the Ca^{2+}-regulated actin–myosin interaction can be accounted for not only by decreased flexibility of actin-bound Tm but also by their influence on the interactions between the middle part of Tm and certain sites of the myosin head.

Introduction

Tropomyosin (Tm) is an actin binding, α-helical coiled-coil protein that binds along the length of actin filament. The current view of thin filament regulation in striated muscle suggests that Tm can be in one of three different positions, or states, on actin: B ('blocked', or calcium-free), C ('closed', or calcium induced) and M (myosin induced, or 'open'), depending on the presence or absence of troponin, myosin and Ca^{2+} [1–4]. The movements of Tm between these positions on the actin surface are believed to play a crucial role in the regulation of the actomyosin interaction. In the absence of Ca^{2+} (B-state) troponin

Abbreviations
S1, myosin subfragment 1; Tm, tropomyosin.

keeps Tm on the actin filament at a position in which it covers the myosin binding sites on actin. When the Ca^{2+} concentration increases, troponin detaches from actin and Tm moves aside to its preferred position on actin (C-state), thus opening the myosin binding areas slightly. Myosin heads first attach to actin 'weakly', i.e. not tightly, and then go into the 'strongly' bound state shifting Tm further away (to the M-state), thus opening neighbor myosin binding sites on adjacent actin monomers.

As with typical coiled-coils, the amino acid sequence of Tm contains a heptad repeat *a-b-c-d-e-f-g* in which residues in *a* and *d* positions are hydrophobic whereas residues in *e* and *g* positions are typically of opposite charge. Residues *a* and *d* of two α-helices interact in a 'knob-into-holes' manner [5] forming a continuous hydrophobic core, which glues the α-helices together. Charged residues in *e* and *g* positions form electrostatic interchain interactions and thus additionally stabilize the coiled-coil structure [4,6,7]. However, the Tm structure is not perfect and contains some structural irregularities such as non-canonical residues in the heptad repeats (e.g. Ala clusters and charged residues in the hydrophobic core) [4,7–10]. These residues which destabilize the coiled-coil structure are predicted to confer conformational mobility, or flexibility, to some parts of the Tm molecule and appear to be important for Tm functioning. One of these parts is the middle of the molecule. Conformational instability of the Tm middle part was demonstrated by different methods (trypsinolysis, CD, differential scanning calorimetry -DSC, as well as an analysis of Tm crystal structures) [9–13].

Lehrer and co-workers [10] found that a particularly unstable region is located in the middle part of the Tm molecule in the vicinity of the non-canonical residue Asp137 (a negatively charged Asp residue in the *d* position that is typically occupied by a hydrophobic residue). The peptide bond between Arg133 and Ala134 was shown to be the most susceptible site to cleavage by trypsin in the full-length Tm [11,12] indicating that the region around Arg133 is the least stable part of the Tm molecule. More recently, attention was attracted to another non-canonical residue nearby, Gly126 in the *g* position instead of a typical charged residue [14]. Importantly, both D137 and G126 are highly conserved, at least in all vertebrate Tm isoforms (Fig. S1). To determine the role of these non-canonical residues in the middle part of Tm, they were replaced with the canonical ones: Asp137 was substituted with Leu by the D137L mutation, introducing a highly preferred hydrophobic residue for the *d* position [10], and Gly126 was replaced with a long charged Arg by the G126R mutation [14]. Both of these replacements were shown to result in stabilization of the Tm molecule as they dramatically reduced the rate of Tm trypsinolysis between Arg133 and Ala134 [10,14]. These mutations increased the thermal stability of Tm as determined by DSC [14–16]. The physiological importance of the middle part of Tm was recently demonstrated in studies with a novel transgenic mouse model expressing cardiac α-Tm with D137L mutation [16].

Interestingly, both mutations stabilizing the middle part of Tm, D137L and G126R, at high calcium concentrations caused a significant increase in the actin-activated ATPase activity of myosin heads in the presence of regulated actin filaments (i.e. thin filaments reconstituted from F-actin, Tm and troponin), although they had no influence on the Tm affinity for actin [10,14]. However, the mechanism of this effect remains unclear.

It was proposed [14] that increased flexibility of the middle part of Tm is attributed to the concerted action of two non-canonical residues, Asp137 and Gly126, as separate substitutions of each of them by canonical residues resulted in similar effects on the structural and functional properties of Tm. In the present work we extended these studies employing various methods and approaches (such as CD, limited proteolysis by trypsin, ATPase measurements, *in vitro* motility assay etc.) to compare structural and functional features of recombinant human striated muscle α-Tm mutants carrying stabilizing substitutions D137L and G126R. Moreover, we studied the combined action of both these substitutions within the same molecule. Our results show that mutations D137L and G126R have similar effects on structural and functional properties of α-Tm, and the joint action of both these mutations is expressed in further significant stabilization of the α-Tm coiled-coil structure and in more pronounced effect on the actin–myosin interaction. We also propose a possible explanation for the physiological effects of these two mutations, according to which their effects on the Ca^{2+}-regulated actin–myosin interaction can be accounted for not only by decreased flexibility of actin-bound Tm but also by the influence of these mutations on the interactions between the central part of Tm and certain sites of the myosin head.

Results

First, we substituted the only Cys residue (Cys190) of α-Tm with an Ala residue to avoid potential complications due to possible disulfide crosslinking of two α-helices of the Tm dimer, as there is evidence that Tm cysteine residues in skeletal and cardiac muscle

cells are in a reduced state [17,18]. This substitution had no appreciable effect on the tryptic digestion of α-Tm [10] and its thermal unfolding measured by DSC (data not shown), and therefore we used this non-Cys control α-Tm C190A as a 'wild-type' protein in all following experiments studying the effects of mutations D137L, G126R and D137L/G126R on structural and functional properties of Tm. It should be noted that in previous work the effects of mutations in the middle part of Tm were studied using either α-Tm C190A [10] or α-Tm WT with reduced SH groups of Cys190 as a reference [14,16]. In the present study we compared the effects of these mutations under the same conditions, using α-Tm C190A as 'α-Tm WT' in its fully reduced state. Note that all these Tm species were recombinant proteins having the Ala-Ser N-terminal extension which is required to mimic the N-terminal acetylation of native Tm (see Experimental procedures).

Stabilization of Tm by mutations D137L, G126R and D137L/G126R

Figure 1A shows typical CD spectra of α-Tm with the classical double negative peaks at 208 nm and 222 nm characteristic for an α-helical coiled-coil protein. The CD spectra recorded at 5 °C were identical for all Tm samples analyzed, α-Tm C190A, D137L/C190A, G126R/C190A and D137L/G126R/C190A. The thermal stability of these Tm species was examined using CD at 222 nm (Fig. 1B). The heat-induced unfolding of all Tm species was fully reversible. In good agreement with previous DSC studies [14–16], the CD results showed that mutations D137L and G126R increase the thermal stability of Tm. Compared with the Tm C190A mutant, both Tm D137L/C190A and Tm G126R/C190A mutants are more stable over the range 30–60 °C (Fig. 1B). For both these mutants the major transition took place at a temperature higher than that for control Tm C190A (42.2 °C) by 3.5 °C (G126R/C190A) and by 3.9 °C (D137L/C190A). However, the most pronounced effect was observed with the mutant α-Tm D137L/G126R/C190A for which the major thermal transition (51.7 °C) is shifted to a higher temperature by more than 9 °C in comparison with Tm C190A and by 5.5–6 °C in comparison with the mutants D137L/C190A and G126R/C190A. Thus, these CD results indicate that mutations D137L and G126R have similar stabilizing effects on the Tm molecule, whereas the combined action of both these mutations results in further significant stabilization of the molecule.

To analyze the stabilizing effects of the D137L, G126R and D137L/G126R mutations on the middle

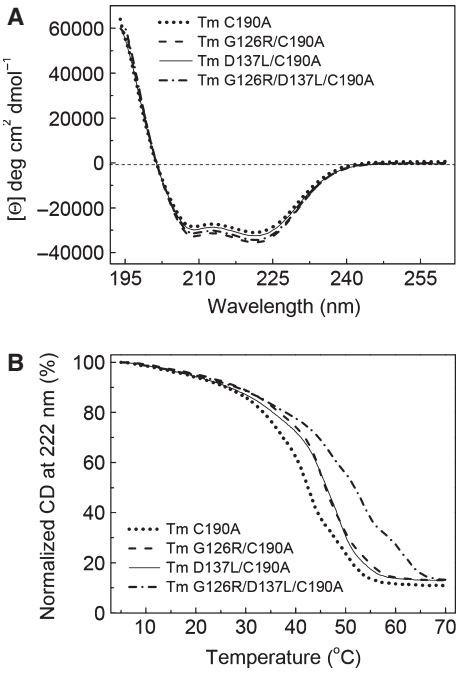

Fig. 1. CD studies on α-Tm species carrying D137L/C190A, G126R/C190A and D137L/G126R/C190A mutations compared with α-Tm C190A. (A) CD spectra in the far-UV region of α-Tm C190A, D137L/C190A, G126R/C190A and D137L/G126R/C190A. The spectra were recorded at 5 °C. Protein concentration was 1.0 mg·mL^{-1} in all cases. (B) Normalized thermal unfolding profiles obtained from the temperature dependence of the α-helix content of these Tm species measured as the ellipticity at 222 nm at a constant heating rate of 1 °C·min^{-1}.

part of Tm, the Tm species were subjected to limited tryptic digestion. Previous studies have shown that trypsin initially cleaves the Tm molecule (either the WT Tm or the C190A mutant) at Arg133 into two fragments [10–12,14], and the mutations D137L or G126R effectively prevent this cleavage [10,14]. Our results show that stabilizing substitutions of non-canonical residues Asp137 and Gly126 similarly reduce the rate of Tm cleavage by trypsin at Arg133, whereas simultaneous substitution of both residues prevents this cleavage even more effectively (Fig. 2). Under the conditions used (a trypsin : Tm weight ratio of 1 : 150), the main band of Tm C190A was fully lost after 12 min of incubation with trypsin, with corresponding appearance of Tm fragments with lower molecular masses indicating cleavage at Arg133 [10]. This cleavage was strongly reduced in the Tm mutants D137L/C190A and G126R/C190A, and it was almost fully prevented in the Tm mutant D137L/G126R/C190A (Fig. 2A). It should be noted, however, that these mutations effectively prevent only the tryptic Tm cleavage at Arg133, but not the cleavage near to

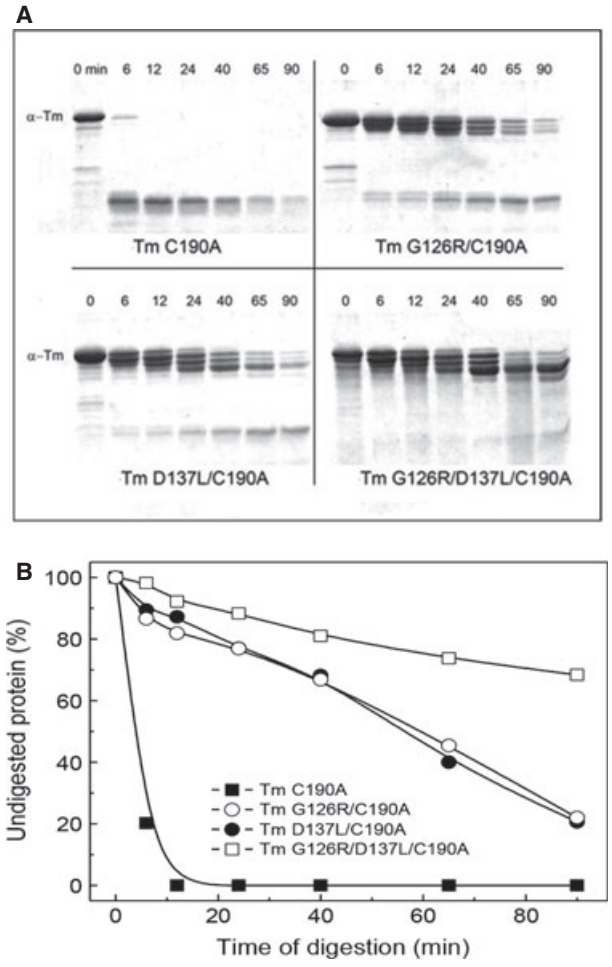

Fig. 2. Tryptic digestion of Tm mutants C190A, D137L/C190A, G126R/C190A and D137L/G126R/C190A at a trypsin : Tm weight ratio of 1 : 150. (A) SDS/PAGE gels. The reaction was quenched at the times indicated. (B) Time course of the Tm cleavage in the middle part of the molecule. Note that 'undigested protein' denotes only the Tm species with no cleavage in the middle part of the molecule, but not the cleavage near to N- and C-termini leading to truncated fragments with molecular masses of 27–32 kDa. Thus, analyzing the scanned images, we summarized the density of the protein bands corresponding to these Tm fragments and denoted the total sum of these fragments by 'undigested protein'.

N- and C-termini, which produces fragments with molecular masses of 27–32 kDa [10]. Analyzing the results (Fig. 2B), we did not take into account these terminal truncations of Tm, and the term 'undigested protein' in the figure denotes only the Tm species with no cleavage at Arg133. It is clearly seen from the figure that double mutation D137L/G126R prevents the tryptic cleavage in the middle part of Tm C190A more effectively than the single mutations D137L or G126R.

Functional effects of mutations D137L/G126R in the middle part of Tm

Following previous studies on the Tm mutants D137L [10] and G126R [14], we also investigated how the double mutation D137L/G126R affects functional properties of Tm. Actin binding properties of D137L/G126R/C190A Tm were studied by co-sedimentation with F-actin and compared with those of C190A Tm (Fig. 3). Both Tm species exhibited similar actin affinity. The $K_{50\%}$ values, corresponding to the Tm concentration at which actin is half-saturated, were 0.58 ± 0.08 μM and 0.67 ± 0.1 μM (mean ± SD) for Tm D137L/G126R/C190A and Tm C190A, respectively. Thus, similar to mutations D137L [10] and G126R [14], the double mutation D137L/G126R had no appreciable influence on the actin affinity for Tm.

Previous studies have shown that Tm dissociates from F-actin on heating, and this process can be monitored with light scattering [14,19–22]. To examine the thermal dissociation of the Tm–F-actin complexes, we measured the temperature dependence of the light

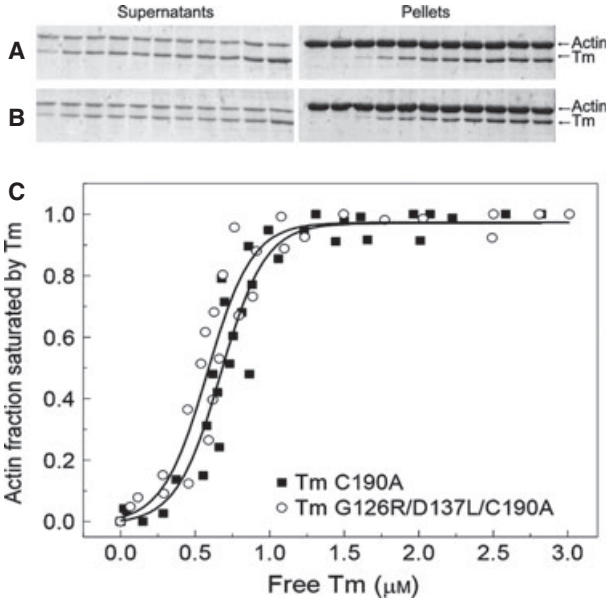

Fig. 3. Affinity of Tm mutants C190A and D137L/G126R/C190A for actin determined by co-sedimentation analysis. (A), (B) SDS gels (15%) used for analysis of actin and Tm C190A (A) or Tm D137L/G126R/C190A (B) in the pellets and supernatants. (C) Plots of the fractional saturation of actin by Tm as a function of the free Tm concentration that was found in the supernatant. The $K_{50\%}$ values, corresponding to the Tm concentration at which half of the actin becomes saturated, are 0.58 ± 0.08 μM and 0.67 ± 0.1 μM for Tm D137L/G126R/C190A and Tm C190A, respectively. These $K_{50\%}$ values are the average ± standard deviation for three experiments; all data points from all experiments are plotted.

scattering for the complexes of phalloidin-stabilized F-actin with Tm mutants C190A, D137L/C190A, G126R/C190A and D137L/G126R/C190A. The decrease in the light scattering intensity reflects dissociation of the Tm–F-actin complexes. The fitted curves to the normalized light scattering changes of dissociation of the Tm–F-actin complexes are shown in Fig. 4. The temperature of the half-maximal dissociation (T_{diss}), i.e. the temperature at which a 50% decrease in the light scattering occurred, was 45.9 °C for C190A Tm, 49.5 °C for G126R/C190A Tm, 51.9 °C for D137L/C190A Tm and 54.0 °C for D137L/G126R/C190A Tm. Thus, both mutations in the Tm middle part, D137L and G126R, significantly increased the T_{diss} value (by 3.6–6.0 °C compared with Tm C190A), whereas the Tm mutant carrying both these stabilizing substitutions, D137L/G126R/C190A, dissociated from F-actin at much higher temperature (by more than 8 °C compared with the C190A Tm). This can be explained, at least partly, by higher thermal stability of this Tm mutant (see Fig. 1B). It seems quite possible that the dissociation temperature of the Tm–F-actin complexes reflects the stability of the complexes, and therefore the most stable (and, probably, less flexible) D137L/G126R/C190A Tm is protected from thermally induced dissociation from F-actin much better than the other Tm species studied.

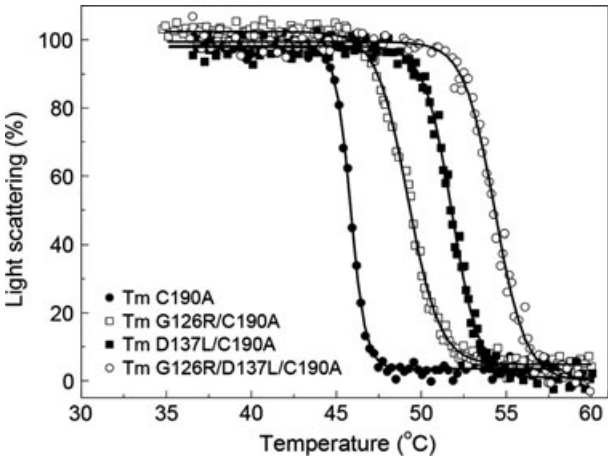

Fig. 4. Normalized temperature dependence of dissociation of the F-actin complexes with Tm C190A, D137L/C190A, G126R/C190A and D137L/G126R/C190A. 100% corresponds to the difference between light scattering of the Tm–F-actin complexes measured at 25 °C and that of pure F-actin stabilized by phalloidin which was temperature independent within the temperature range used. A decrease in the light scattering intensity reflects dissociation of the Tm–F-actin complexes. The samples contained 45 μM F-actin stabilized by phalloidin (60 μM) and 10 μM Tm in 30 mM Hepes, pH 7.3, 100 mM NaCl and 1 mM $MgCl_2$. The heating rate was 1 °C·min^{-1}.

We also studied the effect of the Tm mutant D137L/G126R/C190A on the Ca^{2+}-dependent ATPase of myosin S1 in the presence of the fully regulated thin filaments composed of F-actin, Tm and troponin. At high Ca^{2+}, the D137L/G126R/C190A Tm mutant caused a more than 2-fold increase in the ATPase activity compared with C190A Tm, and this effect was more pronounced than that for the G126R/C190A Tm mutant (Fig. 5A). Similar to the single stabilizing substitution G126R [14], the double mutation D137L/G126R had no appreciable influence on Ca^{2+} sensitivity of the myosin ATPase activated by reconstituted thin filaments (Fig. 5B). The pCa_{50} value (i.e. the negative logarithm of the concentration of free Ca^{2+} at which the ATPase activity is half-maximal) was 6.76 ± 0.07 (here and onwards mean ± SEM) for the filaments containing control C190A Tm,

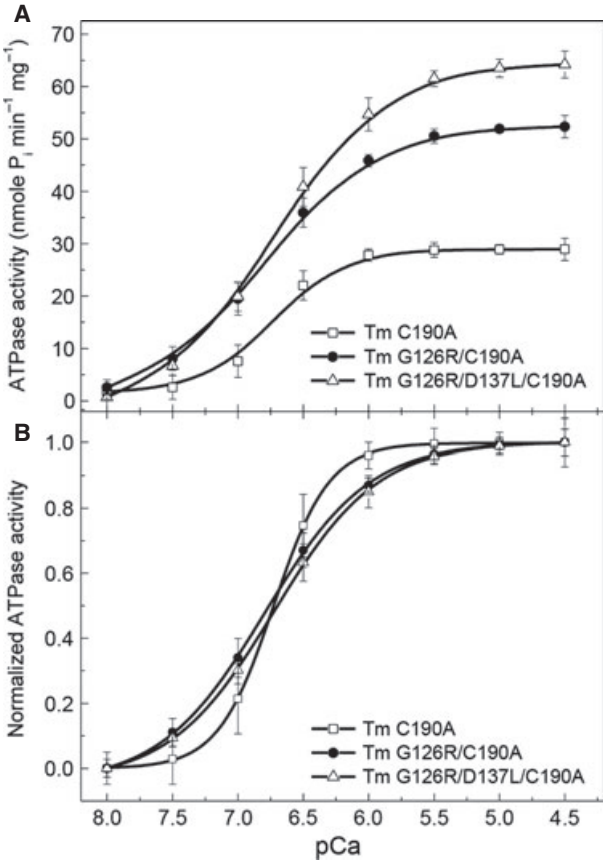

Fig. 5. Effects of Tm mutations G126R/C190A and D137L/G126R/C190A on the Ca^{2+}-dependent actin-activated S1 ATPase of fully regulated reconstituted thin filaments compared with control Tm C190A (A). Samples contained 5 μM F-actin, 2 μM troponin, 2 μM Tm and 2 μM S1. The average standard deviations are indicated with error bars. (B) The same data as in (A) normalized for maximal activity.

6.84 ± 0.09 for the filaments containing G126R/C190A Tm and 6.77 ± 0.06 for the filaments with D137L/G126R/C190A Tm. The Hill cooperativity coefficient *n* was 2.12 ± 0.07 for C190A Tm, 1.16 ± 0.02 for G126R/C190A Tm and 1.16 ± 0.03 for D137L/G126R/C190A Tm.

Importantly, the S1 dependence of the actin-Tm-S1 ATPase showed that the thin filaments containing the Tm mutants D137L, G126R and D137L/G126R had a greater activity than the filaments with Tm C190A not only in the presence of troponin and Ca^{2+} but also in the absence of troponin (Fig. 6A). At low S1 concentrations, both mutations, D137L and G126R, had a lower inhibitory effect on the S1-actin ATPase compared with Tm C190A (this inhibition is a characteristic feature of Tm [23]), whereas the ATPase in the presence of the D137L/G126R mutant was even higher than that with actin alone.

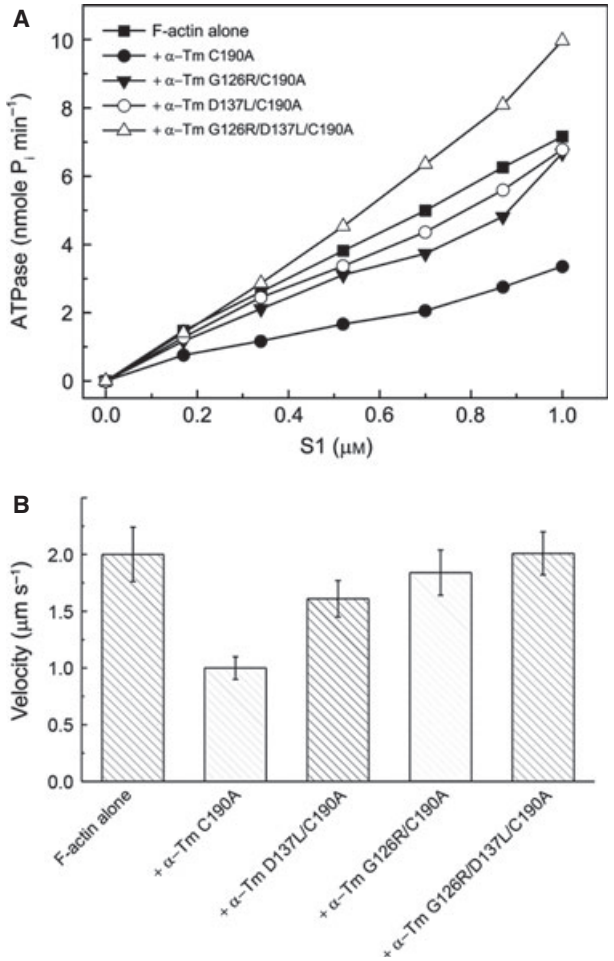

Fig. 6. Effects of Tm mutant constructs C190A, D137L/C190A, G126R/C190A and D137L/G126R/C190A on the acto-S1 ATPase rate (A) and on the sliding velocity of actin filaments in the *in vitro* motility assay (B) in the absence of troponin and Ca^{2+}. (A) Samples contained 5 μM F-actin and 1.2 μM Tm. Other conditions were the same as in Fig. 5A. (B) Average data for two to three experiments with each of the Tm mutants are shown, and vertical bars show the standard deviations of the data between different experiments.

To examine in more detail the effects of the D137L/G126R/C190A mutation on the Tm regulatory properties, we used an *in vitro* motility assay, a highly sensitive method allowing the sliding velocity of the reconstituted thin filaments over the surface covered with immobilized myosin to be monitored. In the absence of troponin, the effects of Tm mutants D137L, G126R and D137L/G126R on the sliding velocity of the actin filaments were similar to those observed with ATPase (Fig. 6A), although less pronounced. Tm C190A substantially suppressed the velocity, while the inhibitory effect of Tm with the D137L or G126R mutations on the velocity was negligible. The Tm double mutant, D137L/G126R, did not suppress the velocity (Fig. 6B). Recently we applied this approach to study the effects of the Tm mutations D137L and G126R on the Ca^{2+}-dependent sliding of the reconstituted thin filaments containing troponin and showed that these mutations not only enhance the maximum sliding velocity of the filaments at high Ca^{2+} concentrations but also increase the Ca^{2+} sensitivity of the velocity by shifting the pCa-velocity curve towards lower Ca^{2+} concentrations [24]. The pCa_{50} values (i.e. pCa at which the sliding velocity was half-maximal) were equal to 6.06 ± 0.04 for the regulated thin filaments containing control Tm C190A, 6.36 ± 0.05 for the filaments containing Tm mutant D137L/C190A, and 6.42 ± 0.03 for the filaments with Tm G126R/C190A [24]. Similar and even more pronounced effects were observed for regulated thin filaments containing the Tm mutant D137L/G126R/C190A (Fig. 7). This mutant caused a significant increase of the sliding velocity of thin filaments at high Ca^{2+} concentrations: 8.2 ± 0.05 μm·s^{-1} compared with 6.05 ± 0.43 μm·s^{-1} for the C190A Tm (Fig. 7A). It also shifted the pCa-velocity curve further towards lower Ca^{2+} concentrations (pCa_{50} = 6.45 ± 0.01 versus 6.03 ± 0.06 for control C190A Tm, Fig. 7B). The Hill cooperativity coefficient *n* was 4.27 ± 0.2 and 2.51 ± 1.06, respectively.

Discussion

The data presented here show that the mutations D137L and G126R similarly stabilize the Tm structure, and the concerted action of both these mutations further stabilizes the Tm molecule. Destabilization of the coiled-coil is necessary for proteolytic cleavage.

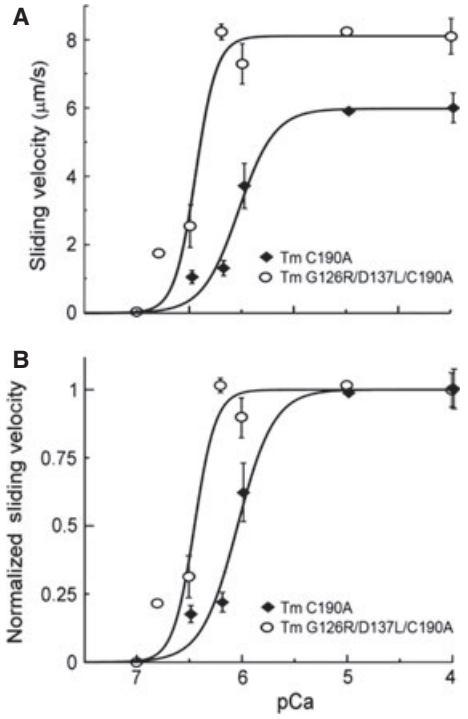

Fig. 7. Effect of the D137L/G126R/C190A Tm mutant construct on the Ca^{2+}-dependent sliding velocity of regulated thin filaments in the *in vitro* motility assay compared with the control C190A Tm construct. (A) Average data for one to three experiments with each of the Tm mutants. Vertical bars show the standard deviations of the data between different experiments. (B) The same data as in (A) normalized for maximal velocity.

The mechanism explaining this Tm destabilization [14] was supposed to include both local chain separation in the vicinity of Asp137 [9] and local unfolding of α-helices in the individual Tm chains caused by non-canonical Gly126. Indeed, stabilizing substitution of either Asp137 or Gly126 was sufficient for thermal stabilization and prevention of the tryptic cleavage of Tm. Moreover, substitution of both these non-canonical residues further increased the Tm stability.

In terms of the actin binding properties, the present results exhibit a high similarity to those obtained previously [10,14]. None of the stabilizing substitutions altered binding of Tm to actin [10,14]. One would expect that these substitutions make the Tm molecule (at least its middle part) more rigid, i.e. less flexible. Thus, the changes in flexibility have no effect on the actin affinity of Tm. However, these substitutions effectively prevent the heat-induced dissociation of the Tm–F-actin complexes; the simultaneous substitution of both Gly126 and Asp137 with the canonical residues was the most effective (Fig. 4). We therefore assume that the decrease in the Tm flexibility stabilizes the Tm–F-actin complexes at high temperature, although having no influence on the actin affinity for Tm at room temperature.

In keeping with previous studies [10,14], our data show that the substitutions in the middle of Tm cause a significant increase in the actin-activated ATPase activity of myosin heads during their interaction with thin filaments at high Ca^{2+} concentrations, although the Ca^{2+} sensitivity of the actomyosin ATPase rate was not significantly affected (Fig. 5). In contrast, our recent [24] and present (Fig. 7B) results clearly indicate that the substitutions D137L, G126R and D137L/G126R significantly increase the Ca^{2+} sensitivity of the sliding velocity of the thin filaments in the *in vitro* motility assay by shifting the pCa-velocity curve towards lower Ca^{2+} concentrations. A discrepancy between the Ca^{2+} sensitivity of the sliding velocity of the thin filaments and of the ATPase rate found here was also observed previously [25,26]. Possible reasons for the discrepancy are as follows. In the previous studies [10,14] the effects of stabilizing substitutions D137L and G126R on the Tm regulatory properties were explained in terms of changed equilibria within the three-state model of thin filament regulation [1] as a shift of the equilibrium from the C (closed) to the M (open) state. However, the pCa dependence of the S1 ATPase rate or filament velocity in the *in vitro* motility assay is determined not only by the Ca^{2+} affinity but also by myosin heads which are strongly bound to actin. These heads push the Tm–troponin system to its open state and facilitate the blocked-to-closed transition of the neighbor region of the thin filaments. Model studies show that a change in the Tm bending stiffness itself can affect the myosin binding properties and the Ca^{2+} sensitivity of the thin filaments [27,28]. Therefore both the Tm stiffness and the distance between the neighbor strongly bound heads are crucial for the pCa sensitivity. Less than one of a hundred actin monomers is occupied by a strongly bound myosin head during ATPase measurement under our experimental conditions. Besides, no mechanical load is present in the ATPase assay. For these reasons the pCa dependence of the ATPase activity is not very cooperative (Fig. 5B) and pCa_{50} does not depend on the stabilizing substitutions in Tm. In contrast, in the motility assay the distance between myosin heads strongly bound to actin is shorter. Also the active myosin heads which propel the thin filament should overcome drag resistance of the weakly bound and 'dead' heads. Under these conditions, the neighbor-to-neighbor interaction of myosin heads with the regulatory system is essential and pCa curves become more cooperative (Fig. 7B), so that the stabilizing Tm mutations affect the pCa dependence of the sliding velocity.

Previously it was proposed that the effects of the D137L and G126R substitutions on the Tm regulatory function can be explained solely by a decrease in flexibility of the Tm molecule caused by these substitutions [10,14]. In this respect, it is rather difficult to explain why Ala substitution for Gly126, which stabilized the α-helix in the middle part of Tm similarly to the Arg substitution, had no effect on the Ca^{2+}-dependent myosin ATPase in the presence of the thin filaments [14].

We suppose that the effects of the stabilizing substitutions in the Tm middle part on the Ca^{2+}-regulated actin–myosin interaction can be accounted for not only by decreased flexibility of actin-bound Tm but rather by an influence of these substitutions on the interactions between Tm and certain sites of a myosin head.

This assumption is based on the analysis of recent data on the structure of the actin–Tm–myosin complex obtained with 8 Å resolution by cryoelectron microscopy and a model built by the docking of crystal structures of actin, myosin S1 and Tm into the cryoelectron microscopy electron density map [29]. An important feature of this model is the presence of direct contacts between Tm located on the surface of the actin filament and some areas of the myosin heads. Since this model has been obtained with a non-muscle myosin-I, we built our model (Fig. 8) by a rigid-body superimposition of the skeletal muscle myosin-II (PDB entry 2MYS) used in our experiments on the position of the Tm-interacting domain of myosin-I used by Behrmann *et al.* [29]. For this purpose we used the atomic structure of chicken myosin-II whereas the experiments were performed with rabbit myosin-II as the residues of interest in these two myosins are identical. In the model we were looking for those residues on the surface of the myosin head which are sufficiently close to the residues at positions 126 and 137 in the middle part of Tm to be able to interact with them. The results of the search are shown in Fig. 8. It turned out that small Gly126 is incapable of any interactions with myosin, whereas the negative charge of Asp137 is close to the positive charge of Arg371 of the myosin head and may interact with it electrostatically (Fig. 8A). Both substitutions in the Tm middle part can affect the Tm–myosin interaction. Due to Arg substitution for Gly126, the side chain of Arg126 in Tm is in the vicinity of that of residue Lys399 on the myosin head, so that an electrostatic repulsion can arise between the positively charged atoms of these residues (Fig. 8B). On the other hand, the electrostatic interaction between Asp137 on Tm and Arg371 of the myosin head is violated by replacing charged residue Asp137 with a neutral Leu residue (Fig. 8B).

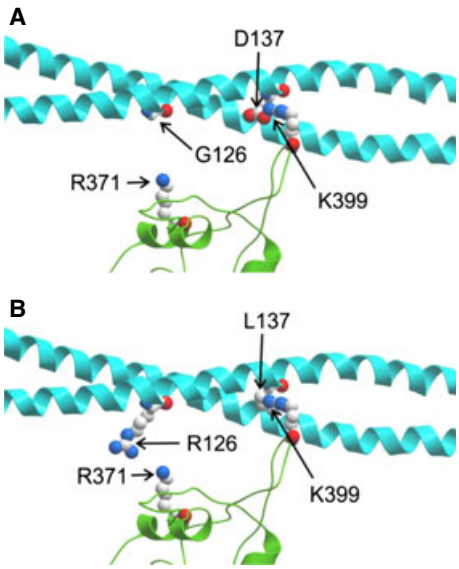

Fig. 8. The structural model of the contact area between Tm bound on the surface of the thin filament and the myosin head (S1) strongly bound to actin. (A) Control Tm containing non-canonical residues D137 and G126 in the middle part of the molecule. (B) Tm mutant with stabilizing substitutions D137L and G126R in the middle part of the molecule. Only some parts of the myosin head adjacent to amino acid residues 126 and 137 in the middle part of Tm are shown. Actin and other parts of myosin and Tm are not shown. The model was obtained from the structure of the actin–myosin–Tm complex [29] (PDB code 4A7H) by superimposing the upper 50-kDa domain of the myosin head of chicken fast skeletal muscle myosin-II (PDB code 2MYS) instead of the same domain of myosin-I used in [29]. Segments of the Tm double α-helix are shown by cyan ribbons; the parts of the head of skeletal muscle myosin-II are green. The non-canonical residues D137 and G126 (A), which were replaced by Leu and by Arg in the G126R/D137L/C190A Tm mutant (B), as well as charged myosin residues K399 and R371 located in close proximity to these Tm residues are shown in the 'ball-and-stick' atomic representation. The distance between the charged atoms of myosin residue K399 and Tm residue R126 (B) in the model was 8.8 Å, and that between myosin R371 and Tm D137 (A) was 4.7 Å. The model and the picture were prepared with ICM-BROWSER (MolSoft, San Diego, CA, USA).

Thus, both substitutions in the Tm middle part, D137L and G126R, should lead to a decrease in the interaction energy of actin-bound Tm with the myosin head strongly bound to actin. The magnitude of the energy reduction is small compared with the energy of strong myosin binding to actin [29] but is comparable with the energy required to move Tm over the surface of the actin filament [30]. In terms of the three-state model of thin filament regulation [1,2] this means that both substitutions, D137L and G126R (and, especially, the combined one, D137L/G126R), would facilitate myosin-induced displacement of Tm over the surface

of the actin filament and promote the transition from the C-state to the M-state. Accordingly, once a myosin head strongly binds actin, these substitutions in Tm should promote the binding of neighbor heads and mechanical work production. This explains, at least partly, the functional effects of the substitutions of either Asp137 or Gly126, or both.

Importantly, the above interpretation can also explain the fact that the replacement of Gly126 in Tm with a small hydrophobic Ala (not the large charged Arg used in the G126R mutant construct) did not affect the S1 ATPase activity in the presence of the thin filaments [14]. Moreover, analyzing the model of the actin–Tm complex [29,31], we found that the residues Asp137 and Gly126 studied here are located rather far from the surface of the actin filament to be able to interact with actin directly. This can explain why the substitutions in the Tm middle part have no influence on actin affinity for Tm.

Our model is based on that of Behrmann *et al.* [29]. Later on another model was proposed [32] to explain the effects of Ala substitutions of conserved surface residues of Tm on its actin affinity and sliding velocity in the *in vitro* motility assay [32,33]. We prefer the model proposed by Behrmann *et al.* [29] to that of Barua *et al.* [32] as in the latter the α-helices of Tm lie outside the electron density map of the cryoelectron microscopy data presented in [29]. It should be noted that the data of Barua *et al.* [32,33] do not contradict our model. In the model by Behrmann *et al.* [29] the Tm residues R125, K128 and V129 (located in the vicinity of G126 and D137) face the actin surface and can interact with both charged and hydrophobic actin residues. One would expect that the replacement of these Tm residues with Ala should weaken the interaction with actin leading to a decrease in the actin affinity as was found by Barua *et al.* [33]. The replacement of charged E150, E156, E163 and E164 Tm residues with Ala was found to depress the sliding velocity in the presence of Ca^{2+}, not affecting the Tm affinity for actin much [32]. Respectively, in the model by Behrmann *et al.* [29] these residues are quite far from the actin surface to affect the affinity essentially. Moreover, in our model the E163 and E164 residues may interact with Arg and Lys residues of a myosin head weakly bound to actin close to the Tm pseudo-repeat 5. The weak-to-strong transition of the head, which is accompanied by its axial and azimuthal tilt with respect to the actin filament, plays an important role in myosin motor function [34,35]. In conclusion, the results presented here shed light on the functional importance of such extraordinary structural features of Tm as the presence of non-canonical residues Asp137 and Gly126 in the middle part of the molecule. Substitutions of these residues with canonical Leu or Arg (D137L and G126R) similarly stabilize the Tm coiled-coil structure, and they both acting together stabilize the Tm molecule further. These two substitutions have a significant effect on the functional properties of Tm: at high Ca^{2+} concentrations they increase the ATPase activity of myosin heads during their interaction with the thin filaments and enhance the sliding velocity of these filaments in the *in vitro* motility assay. They also increase the Ca^{2+} sensitivity of the sliding velocity. It seems at first glance that these substitutions significantly improve the functional properties of Tm making it more effective in realizing its regulatory functions. Recent functional studies with a novel transgenic mouse model expressing cardiac Tm with the D137L mutation have shown that this stabilizing substitution altered *in situ* cardiac function leading to a phenotype similar to dilated cardiomyopathy [16]. These data suggest that extra stabilization of the middle part of Tm as well as the above proposed changes in the interaction of myosin with actin-bound Tm may impair the regulatory functions of Tm. Thus, it seems that the conformational instability (flexibility) of Tm caused by the presence of non-canonical residues Asp137 and Gly126 is essential for proper Tm functioning in the regulation of muscle contraction. The fact that these residues are so conserved in vertebrates (Fig. S1) and are present in virtually all striated and smooth muscle Tm isoforms confirms the importance of this property.

Experimental procedures

Protein preparations

All Tm species used in this work were recombinant proteins that have Ala-Ser N-terminal extension to imitate naturally occurring N-terminal acetylation of native Tm [36]. Human *TPM1* isoform 1 (α-striated Tm) C190A, D137L/C190A, G126R/C190A and D137L/G126R/C190A mutants were prepared in the bacterial expression plasmid pMW172 [37] by PCR-mediated site-directed mutagenesis using Pfu DNA Polymerase (SibEnzyme, Novosibirsk, Russia). The following oligonucleotides were used for mutagenesis: 5′-AAGG CAAAGCTGCCGAGCTTG-3′ for C190A, 5′-GCCCAA AAACTTGAAGAAAAA-3′ for D137L and 5′-GAGTGA GAGACGCATGAAAG-3′ for G126R (mutant codons are underlined). The PCR products were cloned and sequenced to verify the substitutions. The constructs were used to transform the *Escherichia coli* strain BL21(DE3)pLysS, large-scale cultures were grown and overexpression was induced according to standard methods [38]. Bacterial cell

lysates containing recombinant human Ala-Ser α-Tm were heated to 85 °C before clarification by centrifugation at 33 200 ***g*** for 10 min. The resulting supernatant was fractionated by reducing the pH to 4.8, and the recombinant protein was purified by anion exchange chromatography using a HiTrap QXL column (GE Healthcare, Little Chalfont, Buckinghamshire, UK) connected to an FPLC system ProStar (Varian, Mulgrave, Victoria, Australia) with a steady gradient from 0 to 2 M NaCl. Tm concentration was determined spectrophometrically at 280 nm using an $E^{1\%}$ of 2.7 cm^{-1}.

Rabbit skeletal muscle actin, myosin subfragment 1 (S1) and troponin were prepared by established standard methods [39–41]. F-actin polymerized by the addition of 4 mM $MgCl_2$ and 100 mM KCl was further stabilized by the addition of a 1.5-fold molar excess of phalloidin (Sigma Chemical Co., St Louis, MO, USA).

Trypsin digestion

The Tm samples in Hepes buffer (0.5 $mg{\cdot}mL^{-1}$ Tm in 30 mM Hepes, pH 7.3, 100 mM NaCl, 1 mM $MgCl_2$) were treated with L-1-tosylamido-2-phenylethyl chloromethyl ketone-treated trypsin (Worthington) at an enzyme : Tm mass ratio of 1 : 150 at 30 °C. At various times, aliquots were withdrawn, and the reaction was quenched by addition of SDS/PAGE sample buffer containing 5 mM phenylmethanesulfonyl fluoride. Protein compositions of the aliquots were analyzed by SDS-gel electrophoresis.

CD measurements

Far-UV CD spectra of Tm species (1.0 $mg{\cdot}mL^{-1}$) were recorded at 5 °C on a Chirascan circular dichroism spectrometer (Applied Photophysics Ltd., Surrey, UK) in 0.02 cm cells. Thermal unfolding measurements were made by following the molar ellipticity of Tm at 222 nm over the temperature range from 5 °C to 70 °C at a constant heating rate of 1 °C min^{-1}. All measurements were performed in 30 mM Hepes, pH 7.3, 100 mM NaCl, 1 mM $MgCl_2$. The reversibility of the unfolding–refolding process was assessed by reheating the Tm sample directly after it had been cooled from the previous temperature scan. The thermal unfolding of all Tm species was fully reversible.

Co-sedimentation and quantitative electrophoresis

The affinity of Tm for actin was estimated using a co-sedimentation assay according to the general protocol previously described by Kremneva *et al.* [21]. Phalloidin-stabilized F-actin at 10 μM was mixed with increasing concentrations of Tm (0–5 μM) at 20 °C in 30 mM Hepes, pH 7.3, 200 mM NaCl, 1 mM $MgCl_2$, to a final volume of 100 μL. After 30 min incubation the actin was pelleted with any bound Tm by ultracentrifugation at 133 000 ***g*** for 50 min (Beckman airfuge, Beckman Instruments Inc., Palo Alto, CA, USA). Equivalent samples of the pellet and the supernatant were run on SDS/PAGE [42]. Quantification of protein bands was carried out by densitometry using an Astra 6700 scanner (UMAX) and scanned images were analyzed using the IMAGEJ 1.45s software (Scion Corp., Frederick, MD, USA).

Light scattering

Thermally induced dissociation of Tm–F-actin complexes was detected by changes in light scattering at 90° as described earlier [20–22]. The experiments were performed at 350 nm on a Cary Eclipse fluorescence spectrophotometer (Varian Australia Pty Ltd, Mulgrave, Victoria, Australia) equipped with temperature controller and thermoprobes. All measurements were performed at a constant heating rate of 1 °C min^{-1}. Scattering of F-actin solutions containing the same concentration of actin (45 μM) as in the Tm–F-actin samples was measured before the experiments. The scattering of the Tm–F-actin complexes was higher than that of F-actin. When Tm dissociated from F-actin during heating, the value of the light scattering intensity became equal to that of F-actin, because the light scattering of free Tm molecules was negligible [19]. Thus, a temperature-dependent decrease in light scattering intensity of the Tm–F-actin complexes reflects dissociation of Tm from F-actin. The dissociation curves, with temperature dependence of light scattering for F-actin alone deducted, were analyzed by using the ORIGIN software (MicroCal), according to a sigmoidal decay function (Boltzmann). The main parameter extracted from this analysis is T_{diss}, i.e. the temperature at which a 50% decrease in light scattering occurs.

ATPase measurements

Thin filament induced activation of S1 ATPase was assayed by P_i release [43] in a medium containing 10 mM Hepes, 50 mM NaCl, 4 mM $MgCl_2$, 0.1 mM dithiothreitol, pH 7.3. Samples contained 5 μM F-actin; the concentrations of Tm and S1 were as indicated in the captions to Figs 5 and 6A. The ATPase reaction was initiated by addition of 2 mM ATP and stopped after 15 min of incubation at 25 °C by addition of $HClO_4$ to a final concentration of 2.5%. The Ca^{2+} dependence of actin-activated S1 ATPase for the Tm mutants in the presence of the troponin complex (2 μM) was obtained using a 1 mM Ca^{2+}/EGTA buffer system. Calibrated calcium stock solutions were prepared, and equilibrium constants were corrected to the experimental temperature and ionic strength. The MAXCHELATOR program (http://www.stanford.edu/~cpatton/webmaxc/webmaxcS.htm) was used to calculate the free Ca^{2+} concentration.

In vitro motility assay

Experiments and measurement of the sliding velocities of the regulated thin filaments with the *in vitro* motility assay at different Ca^{2+} concentrations were performed as previously described by Shchepkin *et al.* [44]. In brief, a flow cell coated from inside by nitrocellulose was filled with a solution of rabbit skeletal muscle myosin at concentration 0.5 μM (~ 0.2 mg·mL^{-1}) in AB buffer with 500 mM KCl. AB buffer was composed of 25 mM KCl, 25 mM imidazole, 4 mM $MgCl_2$, 1 mM EGTA and 10 mM dithiothreitol, pH 7.5. Then unattached myosin was washed and bovine serum albumin was added into the flow cell. Further non-labeled F-actin in AB buffer with 2 mM ATP was added and incubated for 5 min to block nonfunctional myosin heads. The procedure of assembling regulated thin filaments was as follows. The rhodamine phalloidin labeled actin filaments in a monomer concentration of 10 nM in AB buffer containing 0.1 μM troponin, 0.1 μM tropomyosin, 2 mM ATP and an oxygen scavenger system (3.5 mg·mL^{-1} glucose, 20 μg·mL^{-1} catalase and 0.15 mg·mL^{-1} glucose oxidase) were added into the cell where the thin filaments self-assembled. Free calcium concentrations were set by EGTA/CaEGTA in proportions calculated with the MAXCHELATOR program. Fluorescently labeled thin filaments were visualized with an Axiovert 200 (Carl Zeiss) inverted epifluorescence microscope equipped with a 100 × /1.45 oil-immersion alpha Plan-Fluar objective and an EMCCD iXon-897BV (Andor Technology, Belfast, UK) videocamera. Typically 10 fields by 30 s each were recorded in every flow cell and velocities of 30–100 filaments were measured. The experiments were done at 30 °C; sliding velocities of the filaments were measured using the GMIMPRO software [45]. Experiments for studying the pCa-velocity dependence were repeated two or three times with each of the mutants and the means of individual experiments were fitted to the Hill equation: $v = v_{max}(1 + 10^{n(pCa-pCa50)})^{-1}$, where v and v_{max} are the velocity and maximal velocity obtained at saturating calcium concentration, respectively, pCa_{50} (i.e. calcium sensitivity) is pCa at which half-maximal velocity was achieved, and n is the Hill coefficient. The experiments with unregulated actin filaments (Fig. 6B) were performed under the same conditions, with the only exception that troponin and Ca^{2+} were not added.

Acknowledgements

We are grateful to Dr Bipasha Barua for providing us with the coordinates of the model [29]. This work was supported by the Russian Foundation for Basic Research (grants 12-04-00411 to D.I.L., 11-04-00750 to S.Y.B., 11-04-00908 to A.K.T., 12-04-31328 to D.V.S., and common complex project 13-04-40099-K to D.I.L., S.Y.B. and A.K.T), the Program of Ural Branch RAS (project 12-P-4-1007 to S.Y.B), and the Program 'Molecular and Cell Biology' of the Russian Academy of Sciences (to D.I.L).

References

1 McKillop DF & Geeves MA (1993) Regulation of the interaction between actin and myosin subfragment-1: evidence for three states of the thin filament. *Biophys J* **65**, 693–701.
2 Lehman W, Hatch V, Korman V, Rosol M, Thomas L, Maytum R, Geeves MA, Van Eyk JE, Tobacman LS & Craig R (2000) Tropomyosin and actin isoforms modulate the localization of tropomyosin strands on actin filaments. *J Mol Biol* **302**, 593–606.
3 Lehman W & Craig R (2008) Tropomyosin and the steric mechanism of muscle regulation. *Adv Exp Med Biol* **644**, 95–109.
4 Nevzorov IA & Levitsky DI (2011) Tropomyosin: double helix from the protein world. *Biochemistry (Moscow)* **76**, 1507–1527.
5 Crick FHC (1953) The packing of alpha-helices. Simple coiled-coils. *Acta Crystallogr* **6**, 689–697.
6 Mason JM & Arndt KM (2004) Coiled coil domains: stability, specificity, and biological implications. *ChemBioChem* **5**, 170–176.
7 Hitchcock-DeGregori SE (2008) Tropomyosin: function follows structure. *Adv Exp Med Biol* **644**, 60–72.
8 Minakata S, Maeda K, Oda N, Wakabayashi K, Nitanai Y & Maeda Y (2008) Two-crystal structures of tropomyosin C-terminal fragment 176–273: exposure of the hydrophobic core to the solvent destabilizes the tropomyosin molecule. *Biophys J* **95**, 710–719.
9 Brown JH, Zhou Z, Reshetnikova L, Robinson H, Yammani RD, Tobacman LS & Cohen C (2005) Structure of the mid-region of tropomyosin: bending and binding sites for actin. *Proc Natl Acad Sci USA* **102**, 18878–18883.
10 Sumida JP, Wu E & Lehrer SS (2008) Conserved Asp-137 imparts flexibility to tropomyosin and affects function. *J Biol Chem* **283**, 6728–6734.
11 Pato MD, Mak AS & Smillie LB (1981) Fragments of rabbit striated muscle α-tropomyosin. *J Biol Chem* **256**, 593–601.
12 Ueno H (1984) Local structural changes in tropomyosin detected by a trypsin-probe method. *Biochemistry* **23**, 4791–4798.
13 Sakuma A, Kimura-Sakiyama C, Onoue A, Shitaka Y, Kusakabe T & Miki M (2006) The second half of the firth period of tropomyosin is a key region for Ca^{2+}-dependent regulation of striated muscle thin filaments. *Biochemistry* **45**, 9550–9558.

14 Nevzorov IA, Nikolaeva OP, Kainov YA, Redwood CS & Levitsky DI (2011) Conserved noncanonical residue Gly-126 confers instability to the middle part of the tropomyosin molecule. *J Biol Chem* **286**, 15766–15772.
15 Sumida JP, Hayes D, Langsetmo K & Lehrer SS (2006) Tropomyosin: charge effects in the hydrophobic ridge. *Biophys J* **90** (Suppl.), 193a.
16 Yar S, Chowdhury SAK, Davis RT 3rd, Kobayashi M, Monasky MM, Rajan S, Wolska BM, Gaponenko V, Kobayashi T, Wieczorek DF *et al.* (2013) Conserved Asp-137 is important for both structure and regulatory functions of cardiac α-tropomyosin (α-TM) in a novel transgenic mouse model expressing α-TM-D137L. *J Biol Chem* **288**, 16235–16246.
17 Lehrer SS, Ly S & Fuch F (2011) Tropomyosin is in a reduced state in rabbit psoas muscle. *J Muscle Res Cell Motil* **32**, 19–21.
18 Lehrer SS, Ly S & Fuch F (2011) Tropomyosin is in a reduced state in rat cardiac muscle. *J Muscle Res Cell Motil* **32**, 63–64.
19 Wegner A (1979) Equilibrium of the actin–tropomyosin interaction. *J Mol Biol* **131**, 839–853.
20 Levitsky DI, Rostkova EV, Orlov VN, Nikolaeva OP, Moiseeva LN, Teplova MV & Gusev NB (2000) Complexes of smooth muscle tropomyosin with F-actin studied by differential scanning calorimetry. *Eur J Biochem* **267**, 1869–1877.
21 Kremneva E, Boussouf S, Nikolaeva O, Maytum R, Geeves MA & Levitsky DI (2004) Effects of two familial hypertrophic cardiomyopathy mutations in α-tropomyosin, Asp175Asn and Glu180Gly, on the thermal unfolding of actin-bound tropomyosin. *Biophys J* **87**, 3922–3933.
22 Kremneva E, Nikolaeva O, Maytum R, Arutyunyan AM, Kleimenov SYu, Geeves MA & Levitsky DI (2006) Thermal unfolding of smooth muscle and non-muscle tropomyosin α-homodimers with alternatively spliced exons. *FEBS J* **273**, 588–600.
23 Lehrer SS & Morris EP (1982) Dual effects of tropomyosin and troponin-tropomyosin on actomyosin subfragment 1 ATPase. *J Biol Chem* **257**, 8073–8080.
24 Shchepkin DV, Matyushenko AM, Kopylova GV, Artemova NV, Bershitsky SY, Tsaturyan AK & Levitsky DI (2013) Stabilization of the central part of tropomyosin molecule alters the Ca^{2+}-sensitivity of actin–myosin interaction. *Acta Naturae* **5**, 126–129.
25 Honda H & Asakura S (1989) Calcium triggered movement of regulated actin *in vitro*. A fluorescene microscopy study. *J Mol Biol* **205**, 677–683.
26 Homsher E, Kim B, Bobkova A & Tobacman LS (1996) Calcium regulation of thin filament movement in an *in vitro* motility assay. *Biophys J* **70**, 1881–1892.
27 Smith DA & Geeves MA (2003) Cooperative regulation of myosin–actin interactions by a continuous flexible chain II: actin-tropomyosin-troponin and regulation by calcium. *Biophys J* **84**, 3168–3180.
28 Metalnikova NA & Tsaturyan AK (2013) A mechanistic model of Ca regulation of thin filaments in cardiac muscle. *Biophys J* **105**, 941–950.
29 Behrmann E, Müller M, Penczek PA, Mannherz HG, Manstein DJ & Raunser S (2012) Structure of the rigor actin-tropomyosin-myosin complex. *Cell* **150**, 327–338.
30 Li XE, Tobacman LS, Mun JY, Craig R, Fischer S & Lehman W (2011) Tropomyosin position on F-actin revealed by EM reconstruction and computational chemistry. *Biophys J* **100**, 1005–1013.
31 Sousa DR, Stagg SM & Stroupe ME (2013) Cryo-EM structures of the actin: tropomyosin filament reveal the mechanism for the transition from C- to M-state. *J Mol Biol* **425**, 4544–4555.
32 Barua B, Winkelmann DA, Howard D, White HD & Hitchcock-DeGregoria SE (2012) Regulation of actin–myosin interaction by conserved periodic sites of tropomyosin. *Proc Natl Acad Sci USA* **109**, 18425–18430.
33 Barua B, Pamula MC & Hitchcock-DeGregoria SE (2011) Evolutionarily conserved surface residues constitute actin binding sites of tropomyosin. *Proc Natl Acad Sci USA* **108**, 10150–10155.
34 Taylor KA, Schmitz H, Reedy MC, Goldman YE, Franzini-Armstrong C, Sasaki H, Tregear RT, Poole K, Lucaveche C, Edwards RJ *et al.* (1999) Tomographic 3D reconstruction of quick-frozen, Ca^{2+}-activated contracting insect flight muscle. *Cell* **99**, 421–431.
35 Ferenczi MA, Bershitsky SY, Koubassova N, Siththanandan V, Helsby WI, Panine P, Roessle M, Narayanan T & Tsaturyan AK (2005) The 'roll and lock' mechanism of force generation in muscle. *Structure* **13**, 131–141.
36 Monteiro PB, Lataro RC, Ferro JA & Reinach Fde C (1994) Functional α-tropomyosin produced in *Escherichia coli*. A dipeptide extension can substitute the amino-terminal acetyl group. *J Biol Chem* **269**, 10461–10466.
37 Way M, Pope B, Gooch J, Hawkins M & Weeds AG (1990) Identification of a region in segment 1 of gelsolin critical for actin binding. *EMBO J* **9**, 4103–4109.
38 Studier FW, Rosenberg AH, Dunn JJ & Dubendorff JW (1990) *Methods Enzymol* **185**, 60–89.
39 Spudich JA & Watt S (1971) The regulation of rabbit skeletal muscle contraction. I. Biochemical studies of the interaction of the tropomyosin–troponin complex with actin and the proteolytic fragments of myosin. *J Biol Chem* **246**, 4866–4871.
40 Weeds AG & Taylor RS (1975) Separation of subfragment-1 isoenzymes from rabbit skeletal muscle myosin. *Nature* **257**, 54–56.
41 Greaser ML & Gergely J (1971) Reconstitution of troponin activity from three protein components. *J Biol Chem* **246**, 4226–4233.

42 Laemmli UK (1970) Cleavage of structural proteins during the assembly of the head of bacteriophage T4. *Nature* **227**, 680–685.
43 Panusz HT, Graczyk G, Wilmanska D & Skarzynski J (1970) Analysis of orthophosphate–pyrophosphate mixtures resulting from weak pyrophosphatase activities. *Anal Biochem* **35**, 494–504.
44 Shchepkin DV, Kopylova GV, Nikitina LV, Katsnelson LB & Bershitsky SY (2010) Effects of cardiac myosin binding protein-C on the regulation of interaction of cardiac myosin with thin filament in an *in vitro* motility assay. *Biochem Biophys Res Commun* **401**, 159–163.
45 Mashanov GI & Molloy JE (2007) Automatic detection of single fluorophores in live cells. *Biophys J* **92**, 2199–2211.

Supporting information

Additional supporting information may be found in the online version of this article at the publisher's web site:

Fig. S1. Comparison of amino acid sequence of the middle part of different Tm isoforms.